Structural Engineering and Mechanics, *Vol. 48, No. 4 (2013) 435-453*
DOI: http://dx.doi.org/10.12989/sem.2013.48.4.435

Wind-rain-induced vibration test and analytical method of high-voltage transmission tower

Hong-Nan Li[1], Shun-Yong Tang[1,2] and Ting-Hua Yi[*1]

[1]*Faculty of Infrastructure Engineering, Dalian University of Technology, Dalian 116023, P.R. China*
[2]*China United Engineering Corporation, Hangzhou 310022, P.R. China*

(Received April 23, 2012, Revised September 27, 2013, Accepted October 20, 2013)

Abstract. A new computational approach for the rain load on the transmission tower is presented to obtain the responses of system subjected to the wind and rain combined excitations. First of all, according to the similarity theory, the aeroelastic modeling of high-voltage transmission tower is introduced and two kinds of typical aeroelastic models of transmission towers are manufactured for the wind tunnel tests, which are the antelope horn tower and pole tower. And then, a formula for the pressure time history of rain loads on the tower structure is put forward. The dynamic response analyses and experiments for the two kinds of models are carried out under the wind-induced and wind-rain-induced actions with the uniform and turbulent flow. It has been shown that the results of wind-rain-induced responses are bigger than those of only wind-induced responses and the rain load influence on the transmission tower can't be neglected during the strong rainstorm. The results calculated by the proposed method have a good agreement with those by the wind tunnel test. In addition, the wind-rain-induced responses along and across the wind direction are in the same order of response magnitude of towers.

Keywords: high-voltage transmission tower; rain load; aeroelastic model; wind-rain excitation; wind tunnel test

1. Introduction

The increasing demand for electrical energy of national economy and people's daily life has recently brought significant changes on the formation of electrical energy and the technology of electrical power transmission. A large numbers of electrical power transmission towers have been constructed around the world. Advances on modern construction technology have resulted in increasing application of high-rise transmission towers, large-diameter and long-span conductors in the power transmission system (Li *et al*. 2006). For example, the just completed Zhoushan power transmission tower in China is the world's tallest transmission tower with a total height of 370 m, a weight of 5999 t and a span of 2756 m (Guo *et al*. 2009). The high-voltage transmission tower system is compatible with both high-rise and large-span structural features, such as high-rise tower, large-span conductors, distinct flexibility and geometrical nonlinearity. As one of the most important components in electrical transmission systems, it is a kind of significant lifeline structure. Generally, this structure is sensitive to various kinds of environmental loads (e.g., wind,

*Corresponding author, Professor, E-mail: yth@dlut.edu.cn

http://www.techno-press.org/?journal=sem&subpage=8 ISSN: 1225-4568 (Print), 1598-6217 (Online)

earthquake, rain, and ice accretion). Just take the wind-induced damage for an example, in September 1996, Manitoba Hydro Company, Canada, reported wind damage of about ten million US dollars due to the failure of 19 transmission towers (Shehata *et al*. 2005). When typhoon, 'Maemi', swept Korea in 2003, nine transmission towers collapsed, three were damaged severely and, as a result, many industrial plants and other infrastructure were paralyzed, which caused enormous economic losses (Kepco 2004, Park *et al*. 2007). Investigation of transmission line failures in the America, south-east regions of China, Australia, South Africa, and many other utility organizations has reported that more than 80% of the majority of all weather related line failures were the results of high intensity winds, ranging from fully mature tornadoes to various forms of downbursts and microbursts that are associated with the occurrence of thunderstorms (Dempsey *et al*. 1996). When such failure takes place, it is usually a cascading failure involving a number of adjacent towers along the line. Repair is very costly, in the order of one million dollars per kilometer of the line, leaving aside other costs associated with power disruption and litigation.

In the traditional design of transmission towers, only a few of them have dealt dynamic load to simplify the analysis, and the most research and design attentions on transmission towers have been paid on the actions of static load, impulsive load, equivalent static load, etc. (Yang *et al*. 1996, Yin *et al*. 2009). As this does not match with the exact environmental loads characteristics of transmission towers, the collapse events of the towers frequently occur. In order to overcome the problems, researchers and engineers carried out some dynamic analyses and experiments on the transmission tower system. Gorokhov and his colleagues conducted generalized investigations into towers and poles of overhead power transmission lines. The analysis of climatological, aerodynamic and mechanical data of existing transmission lines had shown that approximately 70% of line failures were caused by overloading their structures during severe wind loads (Kudzys *et al*. 2006). The wind loads used in most codes of practice, standards, and design recommendations for transmission line design are based almost entirely on large-scale wind storms, which may include severe tropical storms such as hurricanes and typhoons (National Electrical Safety Code 1993, Supplement to the National Building Code of Canada 1990). Shehata *et al*. (2005) described a numerical model that could be used to predict the structural performance of a transmission tower as part of a transmission line system under downburst loading. Comparison between the results of the downburst analysis and those due to a normal wind that were typically used in the design reveals the importance of considering high intensity wind loads when attempting the structural design of transmission towers. Previous works by Jamaleddine *et al*. (1993) indicated the adequacy of the commercial software to simulate the ice-shedding problem. Nonlinear analysis was also used by Kalman *et al*. (2007) to calculate the dynamic effects of ice shedding induced by a pulse-type excitation on a single-span overhead line section. The vibration of a two-span section due to ice-shedding from one of the spans had been simulated considering different types of ice by Kollar and Farzaneh (2008). Li *et al* completed a number of research works on seismic problems of a coupled system of long-span transmission towers (Li *et al*. 2002, 2005, Tian *et al*. 2010, Bai *et al*. 2010). He presented simplified computational models and derived the equations of motion for the coupled system of transmission tower-conductors. In order to examine the validity of the presented theoretical models and calculating method, the shaking-table tests of the coupled system of transmission lines and their supporting towers were carried out, and the results indicated that the errors between theoretical and testing results of systemic seismic responses are within the acceptable range in engineering area. Ghobarah *et al*. (1996) investigated the effect of multi-support excitations on the lateral responses of overhead power transmission lines. Transmission towers were modeled by space truss elements and the

cables were modeled by straight two-node elements. In all those studies, longitudinal and transverse responses under uniform excitation and lateral response under multiple-support excitations are obtained.

It has been known from the above state-of-art review that the wind load and ice accretion are conventionally treated as principal governed external loads. In turn, an earthquake is viewed as an incidental load, and other types of loads, especially rain, are poorly defined. However, taking into account the manifold areas where the system is located, several typical collapse events of transmission line systems under the combined actions of severe wind and rainfall conditions have drawn the attention of structural researchers (Eguchi *et al*. 2002). The occurrence of such failures essentially depends on the characteristics i.e. wind intensity, precipitations, incidences of wind and rain, and structural aerodynamic properties. Till now, except for the experimental study of aerodynamic drag of new-design electric power wire under a heavy rain and wind condition by Kikuchi and his coworkers (Kikuchi *et al*. 2003), there are no reports about this phenomenon. Unfortunately, Kikuchi's wind tunnel test only investigated the cross-sectional aerodynamic property rather than expanded into transmission line system. Full-scale tests have also not seen reports because of the difficulty and expense involved. Therefore, it is anticipated that the combined action with severe wind and rainfall could be disclosed, calling the attention of researchers and engineers when attempting the structural design of transmission towers.

The intention of this paper is to establish a rainfall simulation method and reveal the extreme situations of combined action with wind and rainfall that are likely to occur during the designed working life of power transmission lines. The remaining part of the paper is organized as follows. Section 2 presents the wind load and developed rainfall simulation method. Section 3 describes the dynamic response of a pole tower and an antelope's horn tower under the excitation of the separate wind load and combined wind-rain load. In order to confirm the presented method and the results of computer simulation, allow greater confidence in future design work on transmission tower, a physical test is described in section 4 in detail. Section 5 drawn some overall conclusions and some trends of future work are also stated.

2. Wind and rain loads

2.1 Wind load simulation

Currently, the stochastic simulation process for the wind load time history can be roughly divided into the harmonic mode superposition method and the linear filter method. The former is applied here for the wind load simulation. According to the Shinozuka theory (Shinozuka *et al*. 1971), when $N\to\infty$, the random samples of time series of wind load can be simulated by the following

$$u_i(t)=\sum_{l=1}^{i}\sum_{k=1}^{N}\left|H_{il}(\omega_k)\right|\sqrt{2\Delta\omega_k}\cos\left[\omega_k t-\theta_{il}(\omega_k)+\varphi_{lk}\right]\qquad i=1,2,\cdots,m \tag{1}$$

where N means the number for frequencies, i.e. the number of frequency domain data samples, $\theta_{il}(\omega)$ denotes the phase angle between the two different points on the structure and φ_{lk} implies the separate phase angle of uniform distribution between $0\sim2\pi$. According to the approach proposed by Shinozuka (Shinozuka *et al*. 1972), ω_k can be obtained by the following equation

Table 1 Classifications of rainfall amount

Grades	Sprinkle and moderate rainfall	Heavy rainfall	Weak rainstorm	Moderate rainstorm	Strong rainstorm	Maximum
Rainfall (mm/h)	<50	50	100	150	200	709

$$\omega_k = k\Delta\omega_k - \frac{N-l}{N}\Delta\omega_k = (k-1)\Delta\omega_k + \frac{l}{N}\Delta\omega_k \tag{2}$$

2.2 Rain load simulation

2.2.1 Classification of rainfall amount

The classification of rainfall amount given by the meteorological department is based on the average value of 24-hour rainfall, which cannot suitably show the maximum of the rainfall concerned by civil engineers. And it is certainly much less than the maximum rainfall intensity during the rainstorm. In fact, the structure should be able to bear the biggest rainfall intensity force within 24 hours. Thereby, the classification of rainfall amount per hour is taken for tower structural calculation as shown in Table 1 (Li *et al*. 2007).

2.2.2 Spectral distribution of rain particles

A number of observations have indicated that the negative exponent distribution is suitable to describe the raindrop spectra. It is widely used with the Marshall-Palmer exponential distribution, referred to as the M-P spectral distribution (Sheng *et al*. 2003) as follows

$$n(D) = n_0 \exp(-\Lambda D) \tag{3}$$

Where n_0=8×10^{3}sample·m^{-3}·mm^{-1}, Λ denotes the slope factor, which is Λ =4.1I^{-21}, I means the rainfall intensity (mm/h) and D indicates the diameter of a raindrop (mm).

2.2.3 End velocities of raindrops on ground surface

The speed of raindrop gradually increases under gravity during descending, and the air resistance to the raindrop augments at the same time. When the raindrop gravity is equal to the resistance, the raindrop keeps even dropping speed. The speed, V_m, at this time is called as the end velocity on the ground surface, which is given in Li *et al*. (2005)

$$V_m = 10^6\left(\frac{0.787}{D^2} + \frac{503}{\sqrt{D}}\right)^{-1}, \quad D<1.0mm \tag{4}$$

$$V_m = (17.2 - 0.844D)\sqrt{0.1D}, \quad 1.0mm<D<3.0mm \tag{5}$$

$$V_m = \frac{D}{0.113 + 0.0845D}, \quad 3.0mm<D<6.0mm \tag{6}$$

2.2.4 Time history of pressure force of rain load

The speed of raindrop within a very short time becomes zero while it collides with the structure. This interaction between the raindrop and structure follows the Newton's second law (Li *et al*. 2005), and it also conforms to the law of conservation of momentum. The impact force, $F(\tau)$, on the structure during time τ for the raindrop is

$$F(\tau)=\frac{mV_s}{\tau}=\frac{1}{6\tau}\rho\pi d^3V_s \tag{7}$$

where $F(\tau)$ indicates the impact force of raindrop and m means the mass of raindrop, here $m=\rho\pi d^3/6$, V_s is the speed of raindrop, ρ implies the density of raindrop and d is the diameter of raindrop (mm).

The pressure load of a single raindrop impacting on the structure is expressed as follows

$$W_r=\frac{F(\tau)}{A\alpha} \qquad \text{(Unit: Pa)} \tag{8}$$

where A implies the impact area of raindrop, in which $A=\pi d^2/4$, τ indicates the effect time, here $\tau=d/2V_s$ and α means the occupancy rate of raindrop in the air, which can be calculated by the following equation

$$\alpha=\frac{1}{6}\pi d^3N(d) \tag{9}$$

where $N(d)$ is the number of raindrop per unit volume in the air. One can obtain according to Eqs. (7)-(9)

$$W_r=\frac{2}{9}\pi\rho n d^3V_s^2 \tag{10}$$

where n means the density of raindrop number, which is the number of raindrop per unit volume.

In the actual calculation, the pressure of rain load on the structure can be decomposed into the vertical direction and along the wind direction. In the vertical direction, V_s is taken as the free-falling speed, V_m, while along wind direction, V_s is taken as the speed along the wind.

Eq. (10) is rewritten as

$$W_r=\beta_r\mu_rV^2 \tag{11}$$

in which

$$\beta_r=\frac{2}{9}\pi\rho \tag{12}$$

$$\mu_r=nd^3 \tag{13}$$

where β_r is defined as the vibration coefficient for the raindrop and μ_r as the rain-grade coefficient, which is relevant to the diameter of raindrop and density of raindrop number. It increases with the enhancing of the rain-grade (Table 2).

Table 2 Values for μ_r (10^{-6})

Grades	Sprinkle and moderate rain	Heavy rain	Rainstorm	Downpour	Big downpour	Maximum
Rain-grade coefficient	5	6.71	8.17	9.02	10.23	15

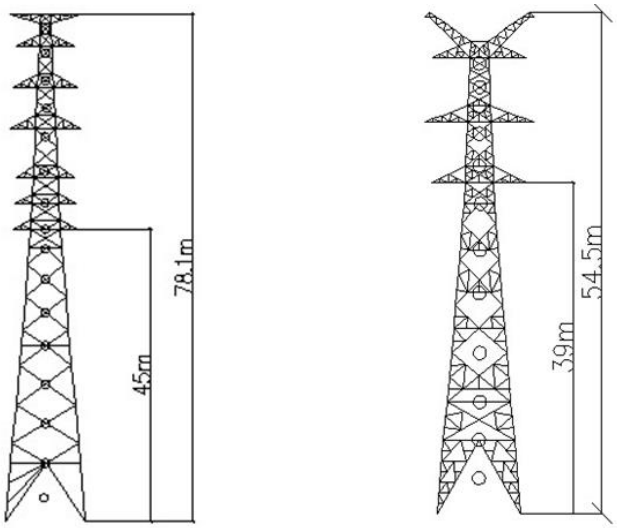

(a) Tower GZIPE (b) Tower YJIRS

Fig. 1 Transmission towers for tests

3. Wind tunnel experiments for transmission towers

3.1 Model design

3.1.1 Similarity criterion

The general similarity in wind tunnel test can be usually met by applying the similarity criterion between the model and prototype (Deng *et al*. 2003). According to the criterion, it is necessary to ensure not only the geometric and rigid similarities between the model and prototype, but also make 6 dimensionless resembling parameters equal between the model and prototype, i.e., the inertial parameter (density ratio), Strouhal number, elastic parameter (Cauchy number), gravity parameter (Froude number), Reynolds number and damping parameters, respectively.

3.1.2 Modeling

Two aeroelastic models of the pole tower (GZ1PE) and the antelope horn tower (RJ1RS) were respectively made for the wind tunnel test. The GZ1PE tower is 78.1 m with its arm 45 m in height; while the YJ1RS tower is 54.5m with its arm 39 m in height. Two lattice towers are made of angle steels, shown in Fig. 1.

There are usually two ways for simulating the rigidity for the model of transmission tower: the centralized stiffness method and discrete stiffness method (Guo *et al*. 2007). In the former approach it respectively simulates the rigidity and geometric shape, which usually uses the brass to

Table 3 Similarity coefficient of tower model

Similarity coefficient	Unit	Similarity ratio of YJ1RS tower	Similarity ratio of GZ1PE tower
Geometry S_l	m	1:32	1:45
Wind velocity S_v	m/s	$1:32^{0.5}$	$1:45^{0.5}$
Frequency S_f	Hz	$32^{0.5}$	$45^{0.5}$
Tensile rigidity S_{EI}	$N.m^2$	$1:32^3$	$1:45^3$
Mass S_m	Kg	$1:32^3$	$1:45^3$
Concentrated load S_F	N	$1:32^3$	$1:45^3$
Displacement Sy	m	1:32	1:45
Acceleration S_a	m/s^2	1	1

(a) Tower GZIPE (b) Tower YJIRS

Fig. 2 Model of towers for the wind and rain induced vibration tests

simulate the stiffness and the ABS slab to simulate the geometric shape. In the later approach each member bar in the model tower is considered as a two-force member. It only utilizes the axial stiffness to simulate the whole stiffness of the model.

The height of the wind tunnel and the dimension of turbulent boundary layer, the scaling parameters of the model are considered according to the height of the prototype tower, as shown in Table 3.

There are many different types of member bars in the tower. However, the difference of them is very small, which can be neglected compared with the difference during modeling for simplification. Therefore, it can merge similar bars into a type when the actual production is made. The member sizes of tower for modeling are shown in Table 4. The wind and rain induced vibration tests for two model towers are shown in Fig. 2.

3.2 Simulation of wind and rain fields

The wind and rain induced vibration tests of the aeroelastic model of transmission tower were done in the wind tunnel of the Shijiazhuang Tiedao University in China. The low-speed test

Table 4 Member size of tower (mm)

Member size of prototype	Member size of model	Geometric shape
2L200×14	Φ0.8×0.12	4.5×0.3
2L200×16		4.5×0.3
L200×24		4.5×0.5
L200×14		4.5×0.3
2L180×14	Φ0.6×0.1	4×0.3
L180×14		4×0.3
L160×14		3.5×0.3
L110×10	Φ0.4×0.08	2.5×0.2
L110×8		2.5×0.2
Other	Φ0.2	

section for the facility is of 4.0 meters wide, 3.0 meters high and 24.0 meters long, and the maximum wind speed is around 30.0 m/s; while the high-speed test section measures 2.2 meters wide, 2.0 meters high and 5.0 meters long, and the maximum wind speed is around 80.0 m/s, in which the wind speed can be continuously adjustable in the two test sections, as shown in Fig. 3(a). The measurement system in this test consists of acceleration sensor, signal measurement and analysis system (DH5922 dynamic signal measurement and analysis system) and computer (data acquisition).

The prototype tower is located in the area of category B of the wind environmental classification in China. The baffle-board and roughness elements on the ground in the wind tunnel are used to simulate the turbulent flow. The height at the reference point is 1.2 m from the bottom. The average wind speed profile, the turbulent intensity profile along the wind and the power spectrum of fluctuating wind were measured, as shown in Figs. 4-6, where n means the frequency, Z indicates the height, U (Z) implies the wind speed at Z point in height, abscissa axis exhibits the Monin coordinate (nZ / U (z)), S denotes the fluctuating wind power spectral density and U^* shows the friction speed. Simulated results showed that the atmospheric boundary layer satisfied the standard requirement. The accurate simulation system of rainfall facilities (Fig. 3(b)) was installed in the low-speed test section, high-speed test section and the first corner, which can simulate all levels of intensity of rainfall from the drizzle to the heavy rain. The wind and rain induced vibration test of the transmission tower was carried out in the low-speed test section.

3.3 Test condition and measuring parameters

3.3.1 Experimental condition

The main contents of the test for the transmission towers include: (1) free vibration characteristics; (2) wind induced responses in the uniform field and turbulent flow field, and (3) both wind and rain induced vibration responses in the uniform field and turbulent flow field. During the experiments, the wind speeds are respectively 2, 3, 4, 5, 6 and 7 m/s, and the rainfalls are 0, 50, 100, 150, 200 mm/h. Sampling time is 60 s, and the sampling frequency is 500 Hz.

3.3.2 Measuring parameters

Three Measurement stations were used in the wind tunnel test. Among them, the sensor 1 and 2

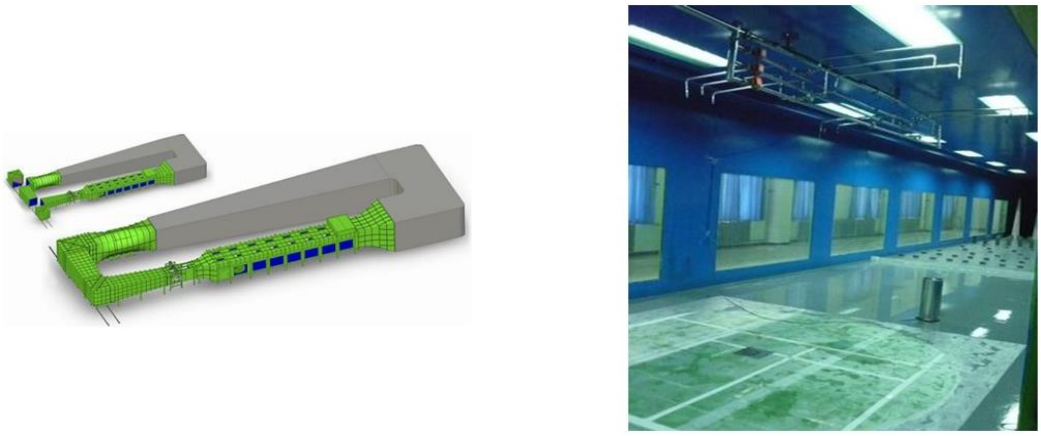

(a) Schematic of the wind tunnel (b) Rainfall facilities in the wind tunnel

Fig. 3 Pictures of wind tunnel

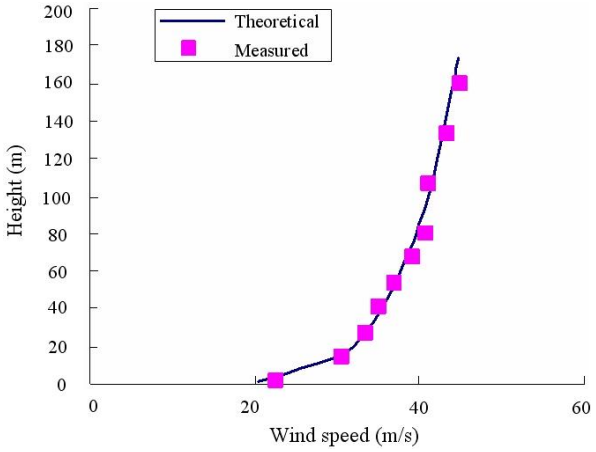

Fig. 4 Mean velocity profile

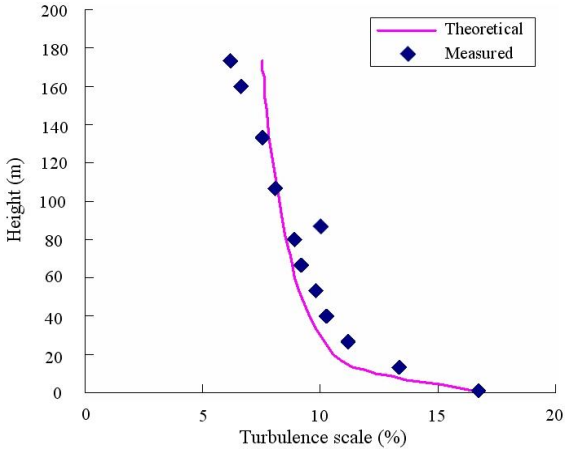

Fig. 5 Turbulent intensity profile

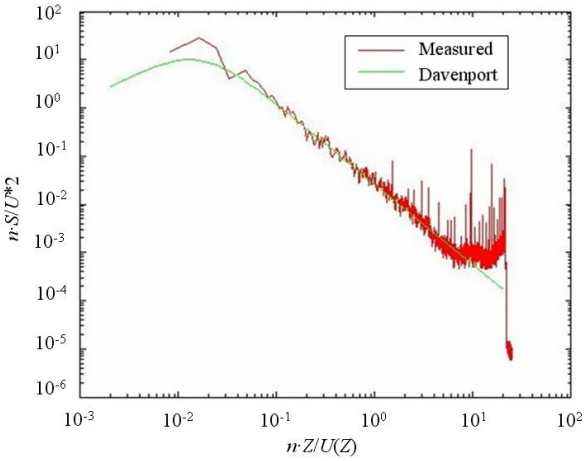

Fig. 6 Power spectrum of fluctuating wind

Table 5 Natural frequencies of experimental models (Hz)

Tower type	Frequency /Hz	Prototype		Expected frequency		Measurement frequency		Relative error /%	
		y	*x*	*y*	*x*	*y*	*x*	*y*	*x*
GZ1PE tower	*f*1	1.57	1.59	10.52	10.53	11.08	11.15	5.3	5.9
	*f*2	3.54	4.21	24.21	29.83	23.26	30.89	4.0	3.6
YJ1RS tower	*f*1	1.81	1.83	10.24	10.35	10.86	10.92	6.1	5.5
	*f*2	2.83	3.98	16.01	22.51	16.93	23.82	5.8	5.9

Note: the *Y* direction is perpendicular to the tower-line plane and *X* direction is parallel to it.

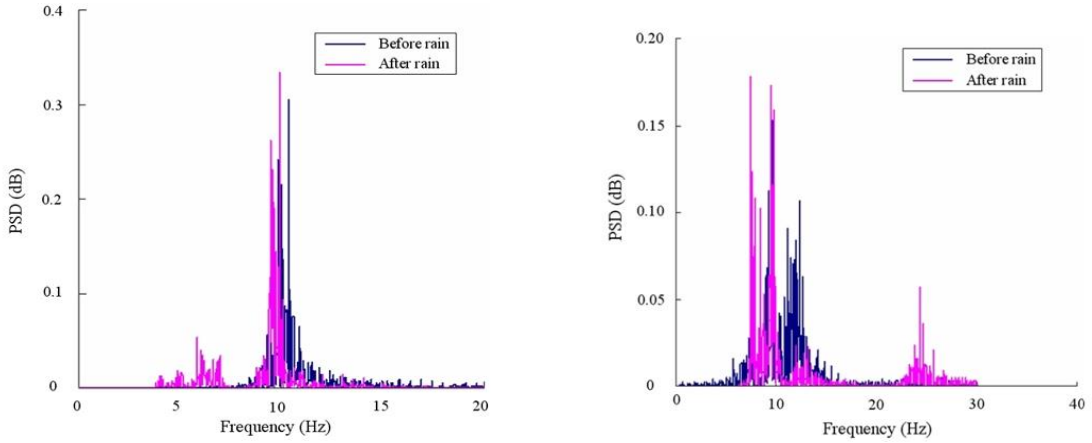

(a) Tower GZIPE (b) Tower YJIRS

Fig. 7 the effect of rainfall for free vibration characteristics

were used to measure the acceleration of *Y* direction at the top of the tower (along the wind), while the sensor 3 for measuring the acceleration of *X* direction (across the wind). The *Y* direction is perpendicular to the tower-line system plane and *X* direction is parallel to the plane. All of the three sensors are arranged at the top of the tower.

4. Experimental results and analyses

4.1 Free vibration

Through free vibration test, natural vibration frequencies for the experimental models were obtained and listed in Table 5. Table 5 shows prototype, expected and measurement values of natural frequencies for experimental models. It can be found that their relative errors are relatively small, less than 7%.

4.2 Effect of rainfall on free vibration characteristics

Fig. 7 shows the free vibration Fourier spectral curves of GZ1PE tower and YJ1RS tower before and after the rainfall, where the blue line represents the Fourier spectral curve before the

Table 6 Mean square roots of acceleration response of GZ1PE tower (m/s^2)

Wind field	Wind speed (m/s)	2	3	4	5	6	7
Uniform flow	Dry surface	0.11325	0.14638	0.17273	0.21969	0.25756	0.31444
	Wet surface	0.11655	0.15099	0.17913	0.22838	0.26932	0.32623
	Increased percent	2.92	3.15	3.71	3.95	4.57	3.75
Turbulent flow	Dry surface	0.18211	0.22818	0.24785	0.27557	0.35044	0.36436
	Wet surface	0.18819	0.23704	0.25822	0.28854	0.36519	0.38025
	Increased percent	3.34	3.88	4.18	4.70	4.21	4.36

Table 7 Mean square roots of acceleration response of YJ1RS tower (m/s^2)

Wind field	Wind speed (m/s)	2	3	4	5	6	7
Uniform flow	Dry surface	0.08864	0.11356	0.13396	0.20518	0.26846	0.34211
	Wet surface	0.09204	0.11716	0.13896	0.21218	0.28046	0.35811
	Increased percent	3.83	3.17	3.73	3.41	4.47	4.68
Turbulent flow	Dry surface	0.15146	0.17908	0.22044	0.30482	0.35307	0.41878
	Wet surface	0.15733	0.18534	0.22857	0.31466	0.36648	0.43176
	Increased percent	3.87	3.50	3.69	3.23	3.80	3.10

rainfall, and the pink line represents the Fourier spectral curve after the rainfall.

It can be seen from the figures that the vibration characteristics of tower have changed after the rainfall. The first-order frequency is smaller than that before the rainfall.

4.3 Dynamic response of transmission towers

4.3.1 Effect of rain wetness on tower surface

Tables 6 and 7 list the mean square roots of acceleration response of the dry and wet surface of GZ1PE tower and YJ1RS tower, respectively.

It can be seen from Tables 6 and 7 that the wind induced response will be increased after the surface of the tower is moistened with water, in which the increased percentage is around 3%-5%. And the increased percentage of acceleration response for two towers is a little similar.

4.3.2 Wind-induced vibration response of towers

Figs. 8 and 9 give the mean square roots of acceleration response of GZ1PE tower and YJ1RS tower under the different wind speeds, respectively.

According to Figs. 8 and 9, some conclusions can be drawn as follows:

(1) The wind-induced vibration responses of towers along and across the wind have the same order of magnitude. It indicates that the wind-induced response of tower across the wind shouldn't be ignored in the tower structural design.

(2) The effects of different wind speeds on the response of tower are quite obvious. With the increase of wind speed, the wind-induced response increases rapidly. It shows that the transmission tower is sensitive to the wind, which is the control load for the design of tower.

(3) The acceleration response of tower in the turbulent flow of wind field is different from that in the uniform flow. And the former is obviously larger than the latter.

(4) The effects of different forms of transmission towers on the wind induced vibration response are slightly different, but not obvious.

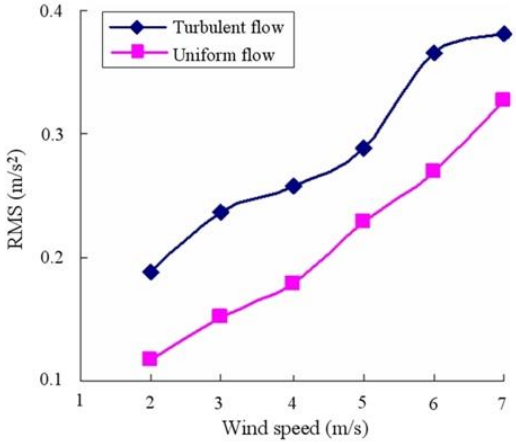

(a) Direction along wind (rainfall r=0 mm/h)

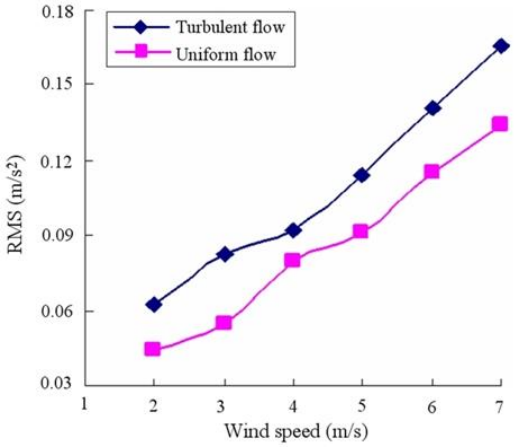

(b) Direction cross wind (rainfall r=0 mm/h)

Fig. 8 Mean square roots of acceleration response of GZ1PE Tower

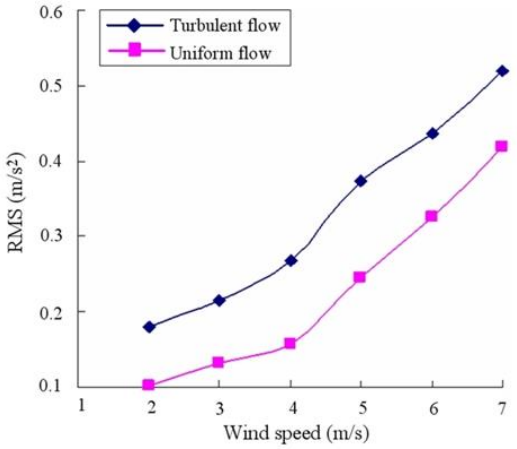

(a) Direction along wind (rainfall r=200 mm/h)

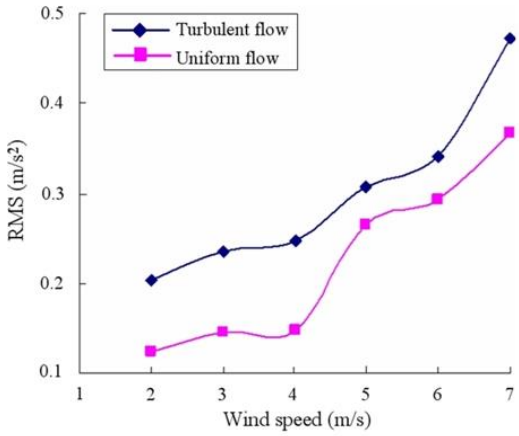

(b) Direction cross wind (rainfall r=200 mm/h)

Fig. 9 Mean square roots of acceleration response of YJ1RS tower

4.3.3 Wind-rain-induced vibration response of towers

Figs. 10 and 11 show the root mean square (RMS) values of acceleration responses of GZ1PE and YJ1RS towers under the different classes of rainfall.

From Figs. 10 and 11, and Tables 8 and 9, the following conclusions can be drawn:

(1) The wind-rain-induced vibration responses of towers along and across the wind have the same order of magnitude. It indicates that the response across the wind shouldn't be ignored in the structural design of the transmission tower.

(2) The effects of different types of rainfalls on the wind-rain-induced tower responses are quite obvious. With the increase of the rainfall intensity, the tower response has an increasing tendency. Increased rates are around with 5%-20%. It shows that the effect of the rainfall on the structure shouldn't be ignored.

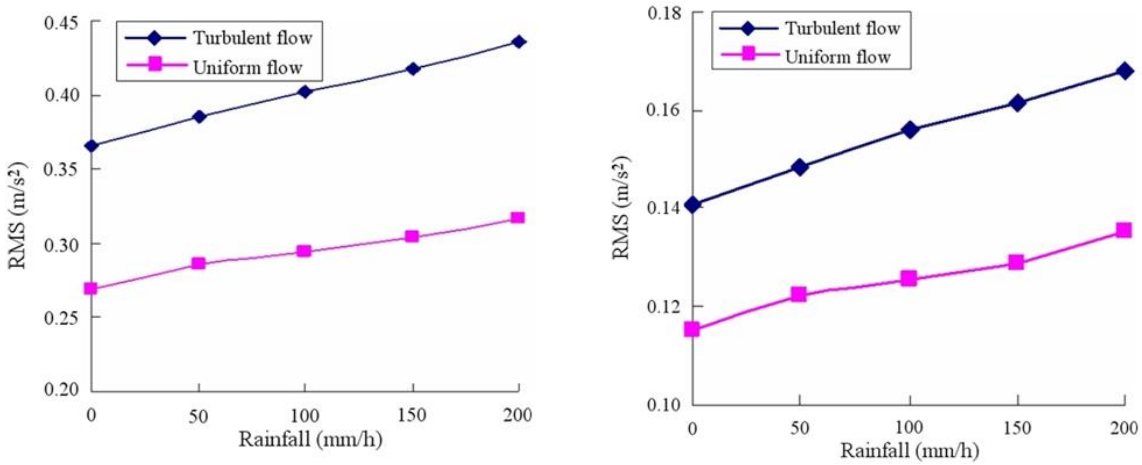

(a) Along wind (wind v=6 m/s) (b) Across wind (wind v=6 m/s)

Fig. 10 Root mean squares value of acceleration response of GZ1PE Tower

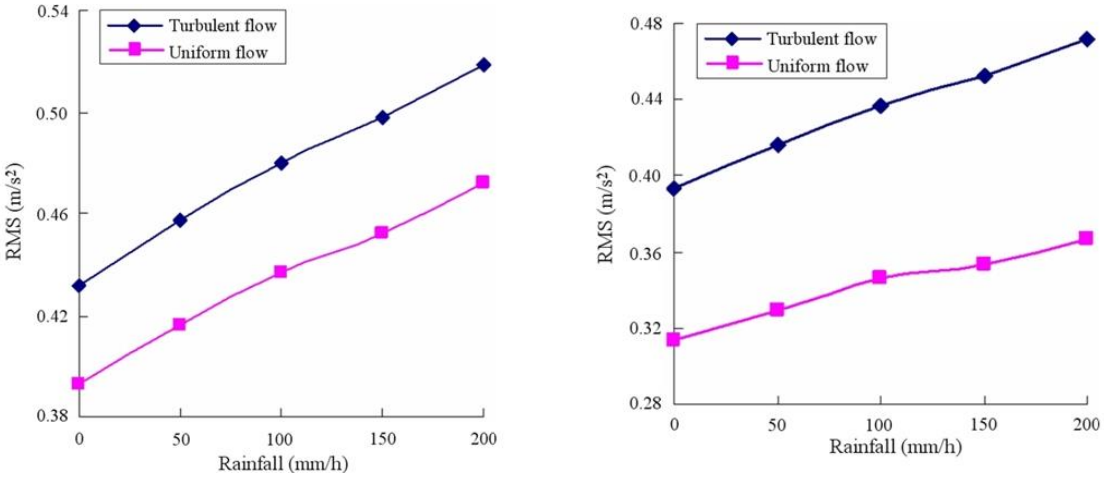

(a) Along wind (wind v=7 m/s) (b) Across wind (wind v=7 m/s)

Fig. 11 Root mean square values of acceleration response of YJ1RS tower

(3) The acceleration response of tower in the turbulent flow of wind-rain field is different from that in the uniform flow. And the former is obviously larger than the latter.

(4) The impacts of different forms of transmission towers on their wind-rain-induced vibration responses are slightly different, but not obvious.

4.4 Comparisons between theoretical and experimental results

Tables 10 and 11 give comparisons between the theoretical and experimental results for the GZ1PE and YJ1RS towers.

Table 8 RMS of acceleration response of GZ1PE tower (reference wind speed v=6.0 m/s)

Wind field	Rainfall (mm/h)	0	50	100	150	200
Turbulent flow	Along the wind	0.36519	0.38586	0.40176	0.41806	0.43593
	Increased percent		5.66	10.01	14.48	19.37
	Across the wind	0.14089	0.14864	0.15587	0.16133	0.16809
	Increased percent		5.50	10.63	14.51	19.31
Uniform flow	Along the wind	0.26932	0.28557	0.29407	0.30356	0.31632
	Increased percent		6.03	9.19	12.71	17.45
	Across the wind	0.11511	0.12211	0.12562	0.12893	0.13546
	Increased percent		6.08	9.13	12.01	17.68

Table 9 RMS of acceleration response of YJ1RS tower (reference wind speed v=7.0 m/s)

Wind field	Rainfall (mm/h)	0	50	100	150	200
Turbulent flow	Along the wind	0.43176	0.45782	0.47989	0.49747	0.51881
	Increased percent		6.04	11.15	15.22	20.16
	Across the wind	0.39266	0.41652	0.43706	0.45239	0.47207
	Increased percent		6.08	11.31	15.21	20.22
Uniform flow	Along the wind	0.35811	0.37735	0.39503	0.40524	0.41929
	Increased percent		5.37	10.31	13.16	17.08
	Across the wind	0.31316	0.32951	0.34598	0.35388	0.36729
	Increased percent		5.22	10.48	13.00	17.29

Table 10 Comparisons between theoretical and experimental results for GZ1PE tower (v=6.0m/s)

Wind field	Rainfalls (mm/h)	0	50	100	150	200
Turbulent flow	Experimental values	0.36519	0.38586	0.40176	0.41806	0.43593
	Theoretical values	0.34508	0.36306	0.37895	0.39364	0.41093
	Errors	5.51	5.91	5.68	5.84	5.73
Uniform flow	Experimental values	0.26932	0.28557	0.29407	0.30356	0.31632
	Theoretical values	0.24691	0.25929	0.26891	0.27694	0.28937
	Errors	8.32	9.20	8.56	8.77	8.52

Table 11 Comparisons between theoretical and experimental results for YJ1RS tower (v=7.0 m/s)

Wind field	Rainfalls (mm/h)	0	50	100	150	200
Turbulent flow	Experimental values	0.43176	0.45782	0.47989	0.49747	0.51881
	Theoretical values	0.41983	0.44358	0.46583	0.48303	0.50173
	Errors	2.76	3.11	2.93	2.90	3.29
Uniform flow	Experimental values	0.35811	0.37735	0.39503	0.40524	0.41929
	Theoretical values	0.33904	0.35604	0.37182	0.38298	0.39625
	Errors	5.33	5.65	5.88	5.49	5.50

From Tables 10 and 11, it can be found that the errors between the experimental and theoretical results are only within 2%-9% for transmission towers, which is satisfactory with computational accuracy.

5. Numerical analysis

5.1 Real towers

There are two real transmission towers for case studies, which are a 500KV pole tower (GZ1PE type) and a 500KV antelope horn tower (YJ1RS type). The GZ1PE tower is 78.1 m high and the YJ1RS tower is 54.5 m high. The construction of towers is all the lattice structure and made of angle steel. Finite element models of towers are shown in Fig. 1.

5.2 Time history of wind load

According to Eq. (1), the parameters of the simulation of the actual fluctuating wind are taken as follows: (1) the ground roughness length Z_0=0.2m; (2) the wind time history length t=300s, time step Δt=0.1s, cutoff frequency ω_u=5HZ, and number of dividing frequency range N=1024; (3) the wind speed spectrum is selected as the Davenport spectrum; (4) the average wind speed at 10 m height: GZ1PE tower: V10=1 0m/s and V10=25 m/s; YJ1RS tower: V10=15 m/s and V10=30 m/s, respectively.

Fig. 12 shows the simulated time history of fluctuating wind at the top points on the tower. To verify the validity and reliability of the simulation method, Eq. (1), the simulated wind field characteristics is compared with the target wind speed spectra shown in Fig. 13. From the figure, it can be seen that the average values of simulated spectrum and target spectrum are very similar, which reveals that the calculating method and parameters chosen are reasonable and effective.

Combined with the simulation of fluctuating wind and the average wind speed, the time history, $V(t)$, of actual wind speed along the tower height can be obtained. Eq. (14) gives the time history of wind load as follows

$$F(t) = \mu_s A V(t)^2 / 1.6 \tag{14}$$

where μ_S is the shape coefficient of the structure，which is taken as 2.5, $V(t)$ is the wind speed and A is the area of the tower to bear wind load.

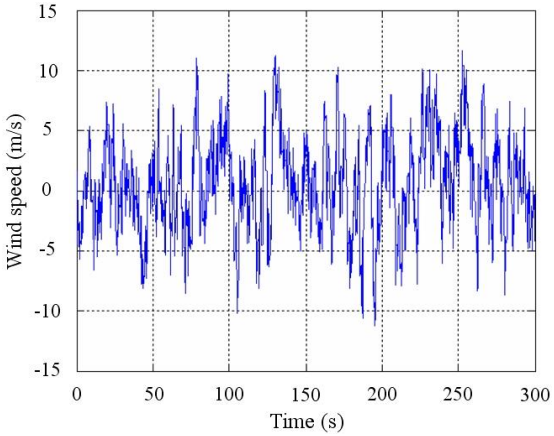

Fig. 12 Simulated fluctuating wind time history

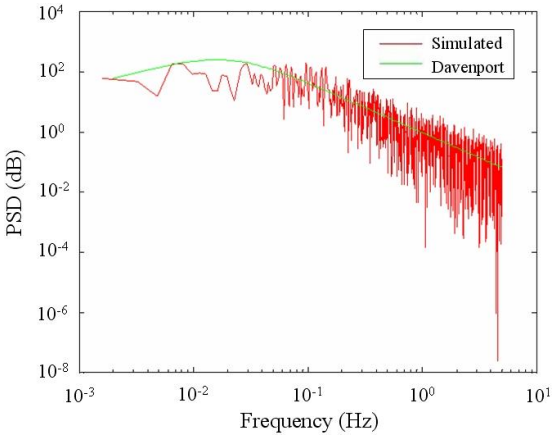

Fig. 13 Comparison between simulated and targets spectra

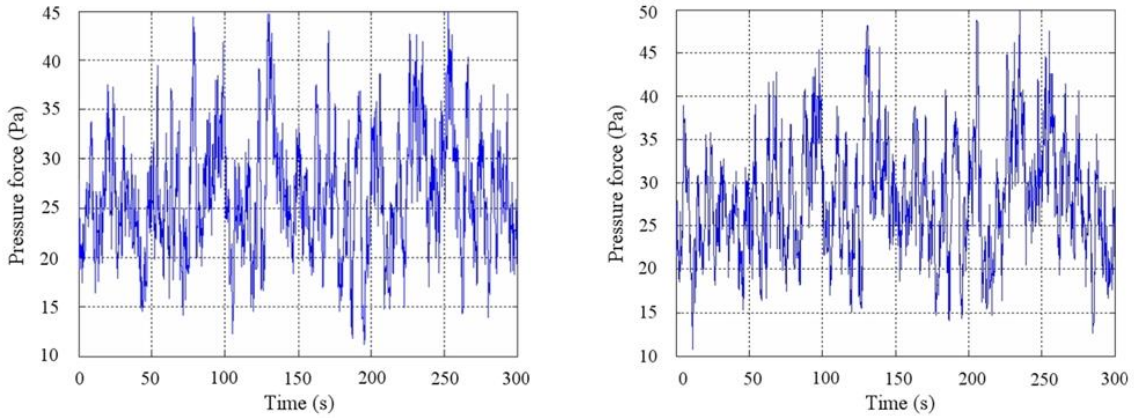

(a) Time history of rainstorm (100 mm/h) (b) Time history of big downpour (200 mm/h)

Fig. 14 Simulated fluctuating rain time history at tower top point

Table 12 Root-mean-square accelerations at the top point of GZ1PE tower along wind direction ($V10$= 25m/s, relative to reference wind speed in wind tunnel, v= 6.0 m/s)

Wind filed	Rain intensities (mm/h)	0	50	100	150	200	709
Turbulent flow	Along wind	0.34508	0.36306	0.37895	0.39364	0.41093	0.42906
	Increased percent		5.21	9.82	14.07	19.08	24.34
Uniform flow	Along wind	0.24691	0.25929	0.26891	0.27694	0.28937	0.29947
	Increased percent		5.01	8.91	12.16	17.20	21.29

Table 13 Root-mean-square accelerations at the top point of YJ1RS tower along wind direction ($V10$=30m/s, relative to reference wind speed in wind tunnel, v=7m/s)

Wind filed	Rain intensities (mm/h)	0	50	100	150	200	709
Turbulent flow	Along wind	0.41983	0.44358	0.46583	0.48303	0.50173	0.52913
	Increased Percent		5.66	10.96	15.05	19.51	26.03
Uniform flow	Along wind	0.33904	0.35604	0.37182	0.38298	0.39625	0.42293
	Increased percent		5.01	9.67	12.96	16.87	24.74

5.3 Time history of rain load

According to the classification of rainfalls and computational approach in Section 2.2, the time histories of rain loads are obtained as shown in Fig. 14.

5.4 Analysis of the Results

The root-mean-square accelerations of dynamic response of the tower are listed in Tables 12 and 13 (where $V10$ means the average wind speed at height of 10 m).

Based on the results of dynamic calculations of towers under different wind speeds and rainfall intensities, some conclusions can be drawn as follows:

(1) Acceleration responses at the tower top point along the wind direction increase with different levels under augment of rainfall intensity. Generally, the increased percentage is in 5%-20%, and even reaches to 26.03% under the extreme situation.

(2) The acceleration response is different from the turbulent and uniform flow fields (different wind fields). The wind-rain-induced responses in the turbulent flow field are bigger than those in the uniform flow field.

6. Conclusions

In this paper, two aeroelastic models of transmission towers are built for the wind tunnel test under wind-rain-induced excitations. A new computational approach for the rain load on the structure of transmission tower is presented to obtain the responses of the system subjected to the wind and rain combined excitations. Through the theoretical and experimental studies, the following conclusions with practical significance can be drawn:

(1) After the surface of the tower is moist, the wind induced response has a tendency to increase, in which the increased percentage is in 3%-6%. The first-order frequency of the tower after the rainfall is smaller than that before the rainfall.

(2) The wind-rain-induced vibration responses of towers along and across the wind have the same order of magnitude. It indicates that the wind-rain-induced response across the wind shouldn't be ignored in the structural design of transmission tower.

(3) The effects of different types of rainfalls on the wind-rain-induced vibration response of towers are sometimes quite obvious. With the augment of rainfall, the wind-rain-induced response has a tendency to increase, in which the increased percentage is around from 5% to 20%. It shows that the effect of rainfall load on the transmission tower should be taken into account in the structural design of transmission tower.

(4) A formula about the rain load pressure is presented in this paper. It provides an approach to study the resistance to the wind and rain for the towers. The results for transmission towers calculated by this proposed method have a good agreement with those of wind tunnel tests. The percentages of errors between the experimental and theoretical results are only within 2%-9%, which is satisfactory with computational accuracy.

Acknowledgements

This research work was jointly supported by the Science Fund for Creative Research Groups of the NSFC (Grant No. 51121005), and the National Natural Science Foundation of China (Grant No. 50638010). In addition, the authors wish to gratefully acknowledge Dr. Guo-Huan Liu for kindly help design of the transmission tower model.

References

American National Standards Institute (ANSI) (1993), "National Electrical Safety Code (NESC)", Accredited Standards Committee.

Bai, F.L., Hao, H. and Li, H.N. (2010), "Seismic response of a steel trussed arch structure to spatially varying earthquake ground motions including site effect", *Adv. Struct. Eng.*, **13**(6), 1089-2103.

Dempsey, D. and White, H. (1996), "Winds wreak havoc on lines", *Transm. Distrib. World*, **48**(6), 32-37.
Deng, H.Z., Zhu, S.Y., Chen, X.M. and Wang, Z.M. (2003), "Wind tunnel investigation on model of long span transmission line system", *J. Tongji Univ*., **31**(2), 132-137.
Eguchi, Y., Kikushi, N., Kawabata, K., Yukinoc, T. and Ishikubo, Y. (2002), "Drag reduction mechanism and aerodynamic characteristics of a newly developed overhead electric wire", *J. Wind Eng. Ind. Aerod*., **90**(4-5), 293-304.
Ghobarah, A., Aziz, T.S. and El-Attar, M. (1996), "Response of transmission lines to multiple support excitations", *Eng. Struct*., **18**(12), 936-946.
Guo, Y., Sun, B.N., Ye, Y., Lo., W.J. and Shen, G.H. (2009), "Frequency-domain analysis on wind-induced dynamic response and vibration control of long span transmission line system", *Acta Aerod. Sinica*, **27**(3), 288-295.
Guo, Y., Sun, B.N., Ye, Y., Shen, G.H. and Lou, W.J. (2007), "Wind tunnel test on aeroelastic model of long span transmission line system", *J. Zhejiang Univ.*, **41**(9), 1482-1486.
Jamaleddine, A., McClure, G., Rousselet, J. and Beauchemin, R. (1993), "Simulation of ice shedding on electrical transmission lines using ADINA", *Comput. Struct*., **47**(4/5), 523-536.
Kalman, T., Farzaneh, M. and McClure, G. (2007), "Numerical analysis of the dynamic effects of shock-load-induced ice shedding on overhead ground wires", *Comput. Struct*., **85**(7/8), 375-384.
Kepco (2004), "*Evaluation of the retrofitting methods for transmission tower body*", Korean Electrical Power Corp.
Kikuchi, N., Matsuzaki, Y., Yukino, T. and Ishida, H. (2003), "Aerodynamic drag of new-design electric power wire in a heavy rainfall and wind", *J. Wind Eng. Ind. Aerod*., **9l**(1), 41-51.
Kollar, L.E. and Farzaneh, M. (2008), "Vibration of bundled conductors following ice shedding", *IEEE Trans. Power Deliv*., **23**(2), 1097-2104.
Kudzys, A. (2006), "Safety of power transmission line structures under wind and ice storms", *Eng. Struct*., **28**(5), 682-689.
Li, G. (2005), "Erosion calculation of raindrops kinetic energy of loess plateaus rainfall", *J. Lanzhou Jiaotong Univ*., **24**(4), 43-45.
Li, H.N. and Bai, H.F. (2006), "High-voltage transmission tower-line system subjected to disaster loads", *Progr. Nat. Sci*., **16**(9), 899-911.
Li, H.N., Ren, Y.M. and Bai, H.F. (2007), "Rain-wind-induced dynamic model for transmission tower", *Proceedings of the CSEE*, **27**(30), 43-48.
Li, H.N., Shi, W.L., Wang, G.X. and Jia, L.G. (2005), "Simplified models and experimental verification for coupled transmission tower-line system to seismic excitations", *J. Sound Vib*., **286**(3), 569-585.
Li, H.N. and Xiao, S.Y. (2002), "Model of transmission tower-pile-soil dynamic interaction under earthquake: in-plane", *ASME PVP.*, **445**, 143-147.
National Research Council of Canada (NRCC) (1990), "Supplement to the National Building Code of Canada", Associate Committee on the National Building Code.
Park, J.H., Moon, B.W., Min, K.W., Lee, S.K. and Kim, C.K. (2007), "Cyclic loading test of friction-type reinforcing members upgrading wind-resistant performance of transmission towers", *Eng. Struct*., **29**(11), 3185-3196.
Shehata, A.Y., Damatty, A. and Savory, E. (2005), "Finite element modeling of transmission line under downburst wind loading", *Finite Elem. Anal. Des*., **42**(1), 71-89.
Sheng, P.X. and Mao, J.T. (2003), *Atmospheric physics*, Beijing University Press, Beijing.
Shinozuka, M. (1971), "Simulation of multivariate and multidimensional random processes", *Acoust. Soc. Am*., **49**(1), 357-368.
Shinozuka, M., Jan C.M. (1972), "Digital simulation of random processes and its applications", *J. Sound Vib*., **25**(1), 111-128.
Tian, L., Li, H.N. and Liu, G.H. (2010), "Seismic response of power transmission tower-line system subjected to spatially varying ground motions", *Math. Probl. Eng*., Article ID 587317, 1-20.
Yang, L., Sun, B. and Ye, Y. (1996), "Calculation of high-voltage transmission tower", *J. Eng. Mech*., **13**(1), 46-51.

Yin, T., Lam, H.F., Chowa, H.M. and Zhub, H.P. (2009), "Dynamic reduction-based structural damage detection of transmission tower utilizing ambient vibration data", *Eng. Struct.*, **31**(9), 19-22.